Editors' Suggestion | Featured in Physics

Brewster-Anomaly Delocalization for Free-Electron Radiation

Zheng Gong,[1,2] Xiangfeng Xi,[1] Hongsheng Chen,[1] Owen D. Miller,[3,*] Stefan Rotter,[2,†] and Xiao Lin[1,‡]

[1]State Key Laboratory of Extreme Photonics and Instrumentation, Zhejiang Key Laboratory of Intelligent Electromagnetic Control and Advanced Electronic Integration, College of Information Science and Electronic Engineering, Zhejiang University, Hangzhou 310027, China

[2]Institute for Theoretical Physics, Vienna University of Technology (TU Wien), Vienna A-1040, Austria

[3]Department of Applied Physics, Yale University, New Haven, Connecticut 06520, USA

(Received 3 June 2026; revised 29 July 2026; accepted 8 September 2026; published 28 October 2026)

Localization effects are central to disordered electronics and photonics. In electronics, Anderson localization governs electron confinement in randomly perturbed lattices. Similarly, its photonic counterpart inhibits light transport via disorder but with a unique exception: Brewster-anomaly delocalization, where the Brewster effect prevents multiple-scattering interference and counteracts the localization. Despite extensive research in electronics and photonics separately, the intricate role of localization effects in interactions between free electrons and light—vital for lasers, accelerators, microscopy and spectroscopy, and quantum information—remains largely unexplored. At the same time, localization effects are widely regarded as a key factor limiting the efficient coupling between free electrons and light in random media. Here, we overcome this key limitation via the unconventional interplay between Brewster-anomaly delocalization and free-electron radiation. In this way, free-electron radiation can be localization-free, intense and directional even in strongly disordered, unengineered multilayers. Essentially, this delocalization-mediated free-electron radiation is remarkably invariant not only to the random-medium configuration, but also to the light frequency and the electron velocity. Our findings unlock new opportunities for particle detectors and achromatic light sources operating in easy-to-fabricate complex media at previously inaccessible frequencies.

DOI: 10.1103/fkp4-9l19

The interaction between free charged particles and matter constitutes a basic pathway to light emission known as charged-particle radiation, for which free-electron radiation [1–8] is a prominent example. The intensity or directionality of this radiation is precisely correlated with the particle kinetic energy or velocity, forming a key principle underpinning particle detectors [9–12]. These detectors not only have facilitated a golden age of discovering new particles [13–15] but also continue the "party of high energy physics" [16] by searching for deviations from the standard model of elementary particles [17–21]. Beyond its established role in particle physics, charged-particle radiation has emerged as a versatile resource in nanophotonics. By granting access to light emission at virtually any frequency, charged-particle radiation empowers a broad spectrum of applications, ranging from tailored light sources [22–25], free-electron lasers [26–28], accelerators [29,30], and magnonic devices [31] to advanced microscopy and spectroscopy [32–35], as well as quantum information technologies [8,36,37].

Central to these advances in particle physics and nanophotonics driven by charged-particle radiation is a paradigm that heavily hinges on modeling free charged-particle interactions with artificial nanostructures. Within this paradigm, structural order typically constitutes a key ingredient. A prime example is free-electron radiation in systems with intrinsic periodicity [38–45] or hidden long-range order [46–48], such as metamaterials, photonic crystals, and photonic quasicrystals [49–52]. Recently, Ref. [53] suggested an alternative route to manipulate free-electron radiation via *judiciously engineered* resonances in pseudorandom media. However, the prohibitive fabrication costs, limited scalability, and stringent tolerance requirements are inherent to structurally ordered designs and engineered resonances. These drawbacks strongly motivate the exploration of free-electron radiation in *unengineered* random media, i.e., systems that enable low-cost, large-scale, and imperfection-robust fabrication.

Nevertheless, operating in the regime of *strong, unengineered* randomness poses a central challenge. The resulting properties (e.g., intensity and directionality) of free-electron radiation are typically regarded as intrinsically random and therefore difficult to predict or control. This apparent link between structural disorder and uncontrolled emission raises a core question: how can free-electron radiation be

*Contact author: owen.miller@yale.edu
†Contact author: stefan.rotter@tuwien.ac.at
‡Contact author: xiaolinzju@zju.edu.cn

 © 2026 American Physical Society

harnessed in strongly disordered media without relying on judicious structural design? From the viewpoint of Anderson localization [54–59], this challenge appears particularly severe, since strong disorder suppresses light transport entirely. As a result, the emitted radiation tends to become localized inside structures with strong disorder, leading to intrinsically low light extraction efficiency. In essence, localization effects impose a key limitation on the effective coupling between free electrons and radiated light in random media.

Here, we overcome this key limitation by exploiting Brewster-anomaly delocalization, which is a unique exception to Anderson localization. Regardless of the structural randomness, the effect of Brewster-anomaly delocalization dictates that the localization length (i.e., the critical length of layered random media required for localization) of p-polarized light diverges at the Brewster angle [60,61]. Ever since its theoretical and experimental identification [60–64], Brewster-anomaly delocalization has been widely studied in random systems incorporating metamaterial composites [65,66], correlated disorder hosting new localization mechanisms beyond the Anderson model [67–69], and emerging time-varying media [70]. These studies have far-reaching implications across diverse areas extending even to biological optics [71,72]. Despite these advances and a long research history in wave control in random media [73–77], Brewster-anomaly delocalization has never been connected to the framework of free-electron radiation. In particular, whether Brewster-anomaly delocalization could impart robust features to free-electron radiation in the presence of strong, unengineered disorder and/or enable its efficient harnessing in random media remains unknown.

Here, we show that free-electron radiation in strongly disordered, unengineered random media can be rendered both intense and directional. On the one hand, Brewster-anomaly delocalization creates intense free-electron radiation by freeing it from otherwise unavoidable localization. On the other hand, the localization-to-delocalization transition from the non-Brewster to the Brewster angle yields directional emission precisely at the Brewster angle. Moreover, rooted in the statistically *invariant* nature of Brewster-anomaly delocalization, the delocalized free-electron radiation we report is robust not only against unengineered variations in the random medium, but also against variations in light frequency and particle velocity. These robust features set our findings apart from *all* known forms of free-electron radiation from random media [46–48,53], such as those based on long-range order or engineered resonances. In short, our findings capture the best of both worlds of free-electron radiation and localization and delocalization effects, yielding intense and directional free-electron emission while maintaining the delocalization-enabled robustness.

Figure 1 provides a conceptual illustration of Brewster-anomaly delocalization for free-electron radiation in strongly disordered, unengineered random media. An electron moving at constant speed penetrates a layered random nanostructure composed of alternating dielectrics I and II [Fig. 1(a)]. Without loss of generality, both dielectrics are assumed to be nondispersive. The unengineered structural randomness is encoded in the thickness of each layer, which is a continuous random variable governed by a probability density function $\mathcal{p}(d_0, \sigma^2)$ (e.g., an exponential distribution), with d_0 and σ denoting the mean value and standard

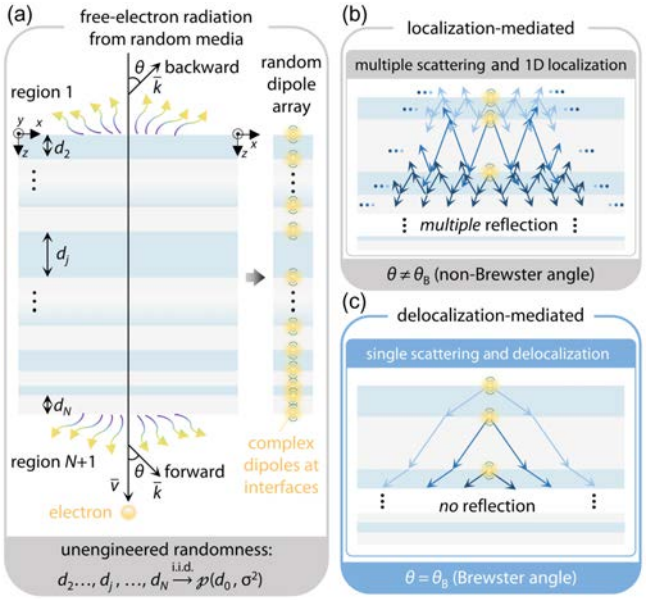


FIG. 1. Conceptual illustration of free-electron radiation from random media mediated by Brewster-anomaly delocalization. (a) Structural schematic. A uniformly moving electron with velocity $\bar{v} = \hat{z}v$ travels perpendicularly through a random multilayer consisting of alternating dielectrics I and II. The layer thicknesses d_j $(j = 2 \ldots N)$ are independent and identically distributed (independently identically distributed) *continuous* random variables with the probability density function $\mathcal{p}(d_0, \sigma^2)$, where d_0 and σ denote the mean value and standard deviation, respectively. As the electron penetrates the random medium, p-polarized light is emitted at each interface. For conceptual simplicity, the total free-electron radiation at the frequency of interest can be modeled as a random array of vertical electric dipoles positioned at each interface, with angular radiation patterns determined by the dielectric relative permittivities ($\varepsilon_{\mathrm{r,I}}$ and $\varepsilon_{\mathrm{r,II}}$) and the electron velocity v. The radiation angle θ is defined as the angle between the wave vector of light and the electron velocity (or the reversed electron velocity) in the substrate region $N + 1$ (or the superstrate region 1). (b),(c) Free-electron radiation in random media mediated by conventional localization effects and Brewster-anomaly delocalization. Unless otherwise specified, throughout the main text we use $\varepsilon_{\mathrm{I}} = 1$, $\varepsilon_{\mathrm{II}} = 2.1$, $v = v_0 = 0.5c < \min(c/\sqrt{\varepsilon_{\mathrm{I}}}, c/\sqrt{\varepsilon_{\mathrm{II}}})$, a total number of interfaces $N = 5 \times 10^4$, working wavelength of light in vacuum $\lambda_0 = 500$ nm, and the thickness of each layer d_j follows an exponential probability density function $p(d_0, \sigma^2) = e^{-d_j/d_0}/d_0$, where $\sigma = d_0 = \lambda_0$.

deviation of this distribution, respectively. Physically, σ/λ_0 quantifies the disorder strength, where λ_0 is the working wavelength of light in vacuum. In the weak-disorder regime (i.e., $\sigma/\lambda_0 \ll 1$), d_0/λ_0 further characterizes the random medium on average as metamaterial-like (i.e., $d_0/\lambda_0 \ll 1$) or as photonic-crystal-like (i.e., $d_0/\lambda_0 \cong 1$) [78]. In this Letter, both d_0/λ_0 and σ/λ_0 are allowed to take arbitrary positive values, placing free-electron radiation in the most general and least predictable regime.

In principle, the resulting free-electron radiation (i.e., transition radiation) is fully coherent, since the quantum-mechanical state of the sample remains unchanged by the electron's penetration [2,5,37,79]. To intuitively appreciate the stochastic nature of free-electron radiation from the random medium, its origin can be modeled as a random array of complex dipoles, all of which are mutually coherent. Specifically, across the broad free-electron radiation spectrum (e.g., from microwave to x-ray), each interface penetrated by the impinging electron behaves as a p-polarized vertical electric dipole at the frequency of interest. The angular pattern of each dipole is determined by the particle velocity and the surrounding media [79–82]. The strong, unengineered disorder then results in a random distribution of the initial dipole phases, in contrast to cases with hidden order or pseudorandomness [46–48,53].

Generally, free-electron radiation is mediated and limited by localization effects [Fig. 1(b)]. As background, localization of light in layered random media is a well-established phenomenon, as demonstrated by numerous experimental studies [57,62–64,83–85]. Following the spirit of light localization and extending it to interactions between free-electrons and light, we decompose the free-electron radiation into plane-wave components characterized by a fixed transverse wave vector (i.e., a fixed emission angle). Each such component propagates through the layered structure as an effectively one-dimensional system, undergoing repeated specular reflections at the interfaces. In the presence of strong disorder, these reflections give rise to multiple scattering whose cumulative effect suppresses transmission and localizes free-electron radiation within the structure, limiting the far-field light extraction efficiency.

In stark contrast, free-electron radiation mediated by Brewster-anomaly delocalization can overcome this limitation [Fig. 1(c)]. At the Brewster angle, radiation emitted at $\theta = \theta_B$ undergoes vanishing reflection at each interface (whether passing from dielectric I to II or vice versa). As a result, the repeated backscattering processes required for localization are suppressed. Consequently, free-electron radiation at the Brewster angle can be effectively modeled as *delocalized* even in the presence of sufficiently strong, unengineered disorder. At this point, a pathway toward realizing Brewster-anomaly delocalization in practice and harnessing it for free-electron radiation is established. First, there is a natural compatibility between Brewster-anomaly delocalization and free-electron radiation, as both can be specific to p-polarized light. Second, owing to the unengineered nature of the system, we simply require sufficient disorder strength, a large number of interfaces, and a proper index contrast for the binary multilayer stack to induce the localization-to-delocalization transition.

We now proceed to show that intense and directional free-electron radiation indeed emerges from random media via Brewster-anomaly delocalization in Fig. 2. The radiation phenomena are classified into three representative regimes [Fig. 2(a)]. The first regime corresponds to conventional localization-mediated free-electron radiation away from the Brewster angle (e.g., $\theta \approx 1.2\theta_B$). When the number of interfaces N is relatively small, the configurationally averaged angular spectral energy density $\langle U \rangle_g$ grows linearly with N, where $\langle \cdot \rangle_g$ represents the geometric average over multiple random configurations. Free-electron radiation emitted in both forward and backward directions (i.e., relative to the direction of electron motion) is summed in $\langle U \rangle_g$. The angular spectral energy density U is numerically

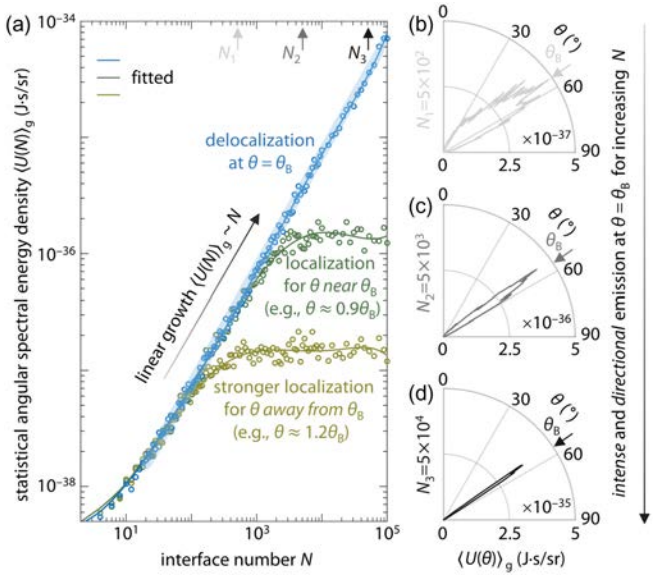


FIG. 2. Intense and directional free-electron radiation from unengineered random media via Brewster-anomaly delocalization. (a) Dependence of the configurationally averaged angular radiation energy density $\langle U(N) \rangle_g$ on the interface number N for various radiation angles. (b)–(d) Angular distribution $\langle U(\theta) \rangle_g$ for various interface numbers. $\langle U \rangle_g = \sqrt[M]{\prod_{i=1}^{M} U_{\text{single},i}} = e^{\sum_{i=1}^{M} \ln(U_{\text{single},i})/M}$ is the geometric average over M configurations of the random medium, where $U_{\text{single},i}$ denotes the ith single configuration. For a large N in (a), the radiation intensity at the non-Brewster angles saturates with increasing interfaces, while it grows linearly at the Brewster angle. This contrasting behavior leads not only to improved intensity but also to directional emission at the Brewster angle in (b)–(d), where N is 500, 5000, and 50 000, respectively. For illustration here and below, we use $M = 100$, the Brewster angle $\theta_B = 55.4°$, and selected angles near and far from the Brewster angle are $49.4° \approx 0.9\theta_B$ and $67.2° \approx 1.2\theta_B$.

obtained by extending Ginzburg and Frank's theory [79,80,86]. The revealed linear growth of $\langle U \rangle_g \sim N$ is consistent with the canonical picture of x-ray transition-radiation particle detectors operated in the weak-absorption regime [10,12]. Yet, when the number of interfaces becomes sufficiently large, localization effects begin to dominate, leading to a pronounced slowdown of the intensity growth and ultimately driving it to saturation. The saturation indicates the balance between the localization-induced suppression and the enhancement originating from an increased number of radiators (i.e., interfaces). In the second regime where the radiation angle is near, but not exactly at the Brewster angle (e.g., $\theta \approx 0.9\theta_B$), the radiation phenomenon shows a similar trend, except that a larger number of interfaces is required to reach the saturation. The larger critical number of interfaces owes its origin to the increased localization length (see also Fig. S1 [86]). For the third regime exactly at the Brewster angle (i.e., $\theta = \theta_B$), the localization length is further increased and divergent, meaning that the localization effect is eliminated entirely. In this scenario, regardless of the number of interfaces, the radiation intensity grows linearly at the Brewster angle, confirming the emergence of intense free-electron radiation from strongly disordered, unengineered random systems.

Putting all three regimes together, we further show in Figs. 2(b)–2(d) that free-electron radiation from strongly disordered, unengineered random media can be highly directional owing to the contrasting mechanisms governing free-electron radiation at the non-Brewster and Brewster angles. In fact, the system size required for delocalized, directional free-electron radiation can be quantitatively estimated from the localization length near the Brewster angle (see also Fig. S2 [86]). As the number of interfaces increases from Figs. 2(b)–2(d), the radiation pattern evolves from a relatively broad and random profile into directional emission with a sharp radiation peak at the Brewster angle. This intense and directional free-electron radiation persists for various disorder distributions (see also Fig. S3 [86]), indicating that our finding is robust against the specific choice of disorder distribution.

To provide deeper insight, we highlight in Fig. 3 that disorder can actually constitute a key factor in improving the directionality of free-electron radiation in random media. To begin with, Fig. 3(a) shows that free-electron radiation is statistically robust against various random-medium configurations, as evidenced by globally consistent radiation features. Averaging over multiple configurations of random media suppresses speckle noise [57,84,87,88], isolating the robust signatures in Fig. 3(b). Closer inspection of the spectra [Figs. 3(a) and 3(b)] reveals two distinct bright stripes. The first appears at low disorder strength $\sigma/\lambda_0 \ll 1$ and vanishes as σ increases, indicating the localization-mediated suppression of free-electron radiation. By contrast, the second bright stripe persists near the Brewster angle even under strong disorder $\sigma/\lambda_0 \gg 1$, confirming the delocalization of free-electron radiation in this regime.

On this basis, we extract from Fig. 3(b) the configurationally averaged radiation intensity $\langle U \rangle_g$ as a function of disorder strength for three representative cases: away from the Brewster angle θ_B (e.g., $\theta \approx 1.2\theta_B$), near θ_B (e.g., $\theta \approx 0.9\theta_B$), and exactly at θ_B (i.e., $\theta = \theta_B$). Far from the Brewster angle, the radiation intensity decays rapidly with increasing disorder before eventually saturating. A similar crossover from decay to saturation arises near the Brewster angle, though the decay rate is slower. Exactly at θ_B, the intensity remains nearly constant across the entire range of disorder. Viewed differently, the disparity between the Brewster and non-Brewster regimes at low disorder and their eventual convergence at high disorder mark the evolution of free-electron radiation from its onset to its steady state. As shown in Figs. 3(d)–3(g), increasing disorder strength enhances the directionality (characterized by the angular width $\Delta\theta$), which eventually remains relatively stable in the strong-disorder regime.

Before closing, we find that the delocalized free-electron radiation mediated by Brewster anomalies exhibits a certain tolerance to variations in material permittivity in Fig. S4 [86] and material loss in Fig. S5 [86]. On this basis, we show in Fig. S6 [86] that realistic low-loss dispersive dielectrics are widely available for constructing layered nanostructures that support Brewster-anomaly-mediated free-electron radiation. The constant-velocity approximation is justified because changes in the electron velocity caused by photon emission are negligible and unwanted inelastic electron scattering is effectively suppressed (see also Fig. S7 [86]).

To conclude, we have proposed a delocalization-mediated mechanism for free-electron radiation in strongly disordered, unengineered random media. This mechanism could enable the emergence of intense, directional free-electron radiation that is robust to variations in unengineered disorder, light frequency, and particle velocity. Our findings overturn the belief that free-electron radiation in strongly disordered, unengineered systems is inherently random and unpredictable, establishing a viable route for controlling free-electron emission in complex photonic environments. Beyond the disorder-immune nature of Brewster-anomaly delocalization for free-electron radiation, its robustness to light frequency and electron velocity (see End Matter, Fig. 4) carries far-reaching implications. First, the achromatic and broadband light emission in random media is highly relevant to laser-based practical applications [89,90] and ultrafast optics [91,92]. Second, the robust response to electron velocity suggests a high degree of tolerance to the noise within the excitation source. The high tolerance paves the way for random radiator-based particle detectors with high signal-to-noise ratios; it also indicates the feasibility of exploring the interplay

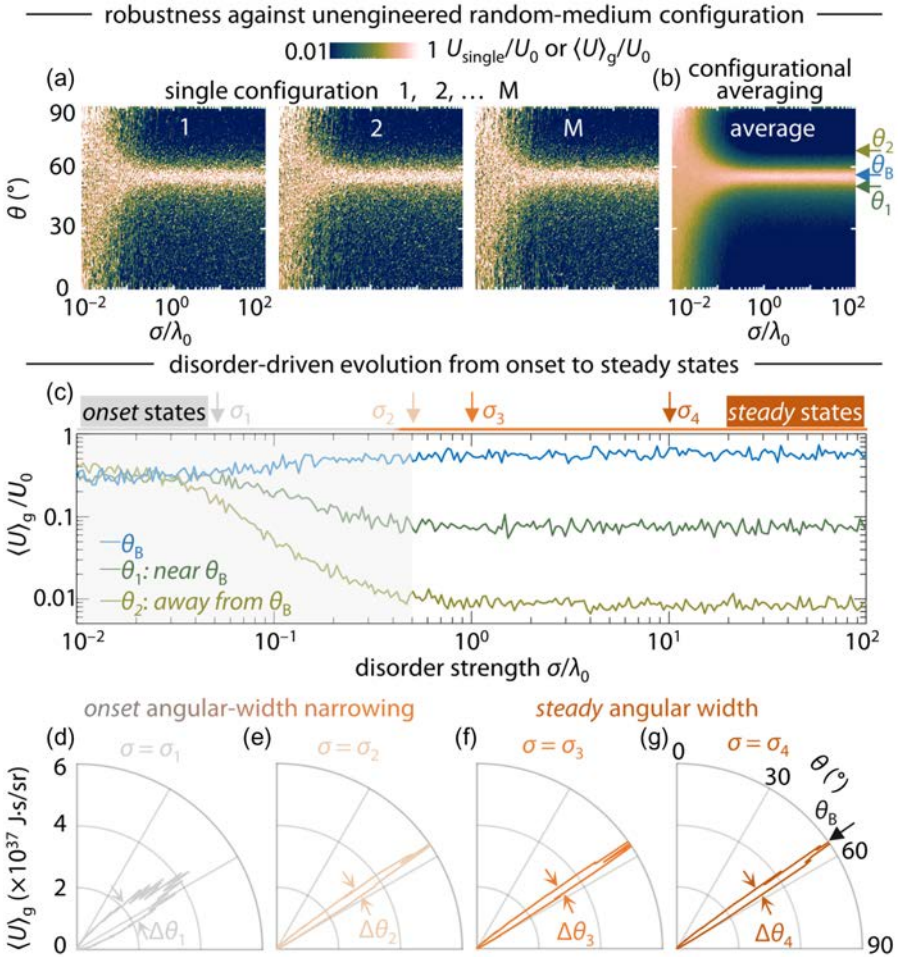


FIG. 3. Disorder-driven evolution of statistically robust free-electron radiation via Brewster-anomaly delocalization. (a),(b) Single-configuration and configurationally averaged angular spectral energy density mapped in the disorder strength σ—radiation angle θ parameter space. The auxiliary normalization factor $U_0 = U_0(\theta)$ is a direct sum of radiation at sequential interfaces; it neglects multiple-scattering and interference effects and is thus independent of σ. (c) Dependence of $\langle U(\sigma)\rangle_g/U_0$ on the disorder strength σ for various emission angles θ. (d)–(g) Angular distribution $\langle U(\theta)\rangle_g$ for various disorder strengths. Locally varied but globally similar free-electron radiation features shown in (a) and (b) indicate its statistical robustness to the random-medium configuration. As the disorder strength increases in (c)–(g), the disorder drives an evolution of free-electron radiation from onset to steady states, respectively characterized by narrowing and stabilizing angular widths (full width at half maximum $\Delta\theta$ of $\langle U(\theta)\rangle_g$).

between Brewster-anomaly delocalization and more complex forms of excitations, including moving or stationary dipoles [93–95], multipoles [96], propagating pulses [31], and realistic electron beam with energy and momentum spread.

Acknowledgments—X. L. acknowledges support partly from National Key Research and Development Program of China under Grant No. 2025YFF0514901, the National Natural Science Foundation of China (NSFC) under Grants No. W2543013 and No. 62475227, and Zhejiang Provincial Natural Science Foundation of China under Grant No. LR26F050002. S. R. acknowledges support by the Austrian Science Fund (FWF) [Grant DOI: 10.55776/PIN7240924] through project META-INCOME. O. D. M. acknowledges support by the Simons Collaboration on Extreme Wave Phenomena Based on Symmetries (Award No. SFI-MPS-EWP-00008530-09). H. C. acknowledges support partly from the National Natural Science Foundation of China (NSFC) under Grants No. U25A20520 and No. 62475228, and the Key Research and Development Program of the Ministry of Science and Technology under Grants No. 2022YFA1404704 and No. 2022YFA1405201. Z. G. acknowledges support from Zhejiang University through the Qiushi Flying Eagle Program and thanks Nazar Pyvovar for helpful discussions on computational techniques.

Data availability—There are no publicly available research data or software supporting this manuscript. Requests for further information or data should be sent to the authors.

[1] A. Friedman, A. Gover, G. Kurizki, S. Ruschin, and A. Yariv, Spontaneous and stimulated emission from quasifree electrons, Rev. Mod. Phys. **60**, 471 (1988).

[2] F. J. Garcia de Abajo, Optical excitations in electron microscopy, Rev. Mod. Phys. **82**, 209 (2010).

[3] H. Hu, X. Lin, and Y. Luo, Free-electron radiation engineering via structured environments, Prog. Electromagn. Res. **171**, 75 (2021).

[4] R. Chen, Z. Gong, J. Chen, X. Zhang, X. Zhu, H. Chen, and X. Lin, Recent advances of transition radiation: Fundamentals and applications, Mater. Today Electron. **3**, 100025 (2023).

[5] C. Roques-Carmes, S. E. Kooi, Y. Yang, N. Rivera, P. D. Keathley, J. D. Joannopoulos, S. G. Johnson, I. Kaminer, K. K. Berggren, and M. Soljačić, Free-electron–light interactions in nanophotonics, Appl. Phys. Rev. **10**, 011303 (2023).

[6] D. Zhang, Y. Zeng, Y. Tian, and R. Li, Coherent free-electron light sources, Photonics Insights **2**, R07 (2023).

[7] X. Lin and H. Chen, Shaping free-electron radiation via van der Waals heterostructures, Light Sci. Appl. **12**, 187 (2023).

[8] R. Ruimy, A. Karnieli, and I. Kaminer, Free-electron quantum optics, Nat. Phys. **21**, 193 (2025).

[9] J. V. Jelley, *Cerenkov Radiation and Its Applications* (Pergamon Press, New York, 1958).

[10] B. Dolgoshein, Transition radiation detectors, Nucl. Instrum. Methods Phys. Res., Sect. A **326**, 434 (1993).

[11] M. Adinolfi, G. Aglieri Rinella, E. Albrecht, T. Bellunato, S. Benson, T. Blake, C. Blanks, S. Brisbane, N. H. Brook, and M. Calvi, Performance of the LHCb RICH detector at the LHC, Eur. Phys. J. C **73**, 2431 (2013).

[12] C. W. Fabjan and H. Schopper, *Particle Physics Reference Library: Volume 2: Detectors for Particles and Radiation* (Springer Nature, Cham, 2020).

[13] O. Chamberlain, E. Segrè, C. Wiegand, and T. Ypsilantis, Observation of antiprotons, Phys. Rev. **100**, 947 (1955).

[14] J. J. Aubert, U. Becker, P. J. Biggs, J. Burger, M. Chen, G. Everhart, P. Goldhagen, J. Leong, T. McCorriston, and T. G. Rhoades, Experimental observation of a heavy particle *J*, Phys. Rev. Lett. **33**, 1404 (1974).

[15] G. Arnison, A. Astbury, B. Aubert, C. Bacci, G. Bauer, A. Bézaguet, R. Böck, T. J. V Bowcock, M. Calvetti, and T. Carroll, Experimental observation of isolated large transverse energy electrons with associated missing energy at s = 540 GeV, Phys. Lett. **122B**, 103 (1983).

[16] S.-H. H. Tye, Supplement to the "Giant Collider in China" debate: Background on Prof. CN Yang's opinion on high-energy physics, Int. J. Mod. Phys. A **31**, 1630056 (2016).

[17] S. Weinberg, A model of leptons, Phys. Rev. Lett. **19**, 1264 (1967).

[18] M. K. Gaillard, P. D. Grannis, and F. J. Sciulli, The standard model of particle physics, Rev. Mod. Phys. **71**, S96 (1999).

[19] ATLAS Collaboration, Observation of a new particle in the search for the standard model Higgs boson with the ATLAS detector at the LHC, Phys. Lett. B **716**, 1 (2012).

[20] A detailed map of Higgs boson interactions by the ATLAS experiment ten years after the discovery, Nature (London) **607**, 52 (2022).

[21] D. P. Aguillard, T. Albahri, D. Allspach, A. Anisenkov, K. Badgley, S. Baeßler, I. Bailey, L. Bailey, V. A. Baranov, and E. Barlas-Yucel, Measurement of the positive muon anomalous magnetic moment to 0.20 ppm, Phys. Rev. Lett. **131**, 161802 (2023).

[22] F. Liu, L. Xiao, Y. Ye, M. Wang, K. Cui, X. Feng, W. Zhang, and Y. Huang, Integrated Cherenkov radiation emitter eliminating the electron velocity threshold, Nat. Photonics **11**, 289 (2017).

[23] C. Roques-Carmes, S. E. Kooi, Y. Yang, A. Massuda, P. D. Keathley, A. Zaidi, Y. Yang, J. D. Joannopoulos, K. K. Berggren, and I. Kaminer, Towards integrated tunable all-silicon free-electron light sources, Nat. Commun. **10**, 3176 (2019).

[24] Y. Yang, C. Roques-Carmes, S. E. Kooi, H. Tang, J. Beroz, E. Mazur, I. Kaminer, J. D. Joannopoulos, and M. Soljačić, Photonic flatband resonances for free-electron radiation, Nature (London) **613**, 42 (2023).

[25] T. Li, F. Liu, Y. Chen, X. Xiong, K. Cui, X. Feng, W. Zhang, and Y. Huang, On-chip Cherenkov radiation tuning in 3.2–14 THz, Nat. Commun. **16**, 7921 (2025).

[26] W. Wang, K. Feng, L. Ke, C. Yu, Y. Xu, R. Qi, Y. Chen, Z. Qin, Z. Zhang, and M. Fang, Free-electron lasing at 27 nanometres based on a laser wakefield accelerator, Nature (London) **595**, 516 (2021).

[27] M. Galletti, R. Assmann, M. E. Couprie, M. Ferrario, L. Giannessi, A. Irman, R. Pompili, and W. Wang, Prospects for free-electron lasers powered by plasma-wakefield-accelerated beams, Nat. Photonics **18**, 780 (2024).

[28] R. Pompili, D. Alesini, M. P. Anania, S. Arjmand, M. Behtouei, M. Bellaveglia, A. Biagioni, B. Buonomo, F. Cardelli, and M. Carpanese, Free-electron lasing with compact beam-driven plasma wakefield accelerator, Nature (London) **605**, 659 (2022).

[29] T. Chlouba, R. Shiloh, S. Kraus, L. Brückner, J. Litzel, and P. Hommelhoff, Coherent nanophotonic electron accelerator, Nature (London) **622**, 476 (2023).

[30] A. Cho, Laser-powered accelerators, compact and cheap, get real, Science **387**, 459 (2025).

[31] I. A. Filatov, P. I. Gerevenkov, A. V Azovtsev, V. A. Kovaleva, N. E. Khokhlov, and A. M. Kalashnikova, Magnon-Cherenkov effect from a picosecond strain pulse, Nat. Phys. **22**, 252 (2026).

[32] K. Wang, R. Dahan, M. Shentcis, Y. Kauffmann, A. Ben Hayun, O. Reinhardt, S. Tsesses, and I. Kaminer, Coherent interaction between free electrons and a photonic cavity, Nature (London) **582**, 50 (2020).

[33] O. Kfir, H. Lourenço-Martins, G. Storeck, M. Sivis, T. R. Harvey, T. J. Kippenberg, A. Feist, and C. Ropers, Controlling free electrons with optical whispering-gallery modes, Nature (London) **582**, 46 (2020).

[34] J.-W. Henke, A. S. Raja, A. Feist, G. Huang, G. Arend, Y. Yang, F. J. Kappert, R. N. Wang, M. Möller, and J. Pan, Integrated photonics enables continuous-beam electron phase modulation, Nature (London) **600**, 653 (2021).

[35] Y. Yang, J.-W. Henke, A. S. Raja, F. J. Kappert, G. Huang, G. Arend, Z. Qiu, A. Feist, R. N. Wang, and A. Tusnin, Free-electron interaction with nonlinear optical states in microresonators, Science **383**, 168 (2024).

[36] A. Feist, G. Huang, G. Arend, Y. Yang, J.-W. Henke, A. S. Raja, F. J. Kappert, R. N. Wang, H. Lourenço-Martins, and

Z. Qiu, Cavity-mediated electron-photon pairs, Science **377**, 777 (2022).
[37] A. Preimesberger, D. Hornof, T. Dorfner, T. Schachinger, M. Hrtoň, A. Konečná, and P. Haslinger, Exploring single-photon recoil on free electrons, Phys. Rev. Lett. **134**, 096901 (2025).
[38] F. J. Garcia de Abajo, N. Zabala, A. Rivacoba, A. G. Pattantyus-Abraham, M. O. Wolf, and P. M. Echenique, Cherenkov effect as a probe of photonic nanostructures, Phys. Rev. Lett. **91**, 143902 (2003).
[39] C. Luo, M. Ibanescu, S. G. Johnson, and J. D. Joannopoulos, Cerenkov radiation in photonic crystals, Science **299**, 368 (2003).
[40] Y. Zhang, Z. D. Gao, Z. Qi, S. N. Zhu, and N. B. Ming, Nonlinear Čerenkov radiation in nonlinear photonic crystal waveguides, Phys. Rev. Lett. **100**, 163904 (2008).
[41] Z. Wang, K. Yao, M. Chen, H. Chen, and Y. Liu, Manipulating Smith-Purcell emission with babinet metasurfaces, Phys. Rev. Lett. **117**, 157401 (2016).
[42] X. Lin, S. Easo, Y. Shen, H. Chen, B. Zhang, J. D. Joannopoulos, M. Soljačić, and I. Kaminer, Controlling Cherenkov angles with resonance transition radiation, Nat. Phys. **14**, 816 (2018).
[43] X. Lin *et al.*, A Brewster route to Cherenkov detectors, Nat. Commun. **12**, 5554 (2021).
[44] A. Dikopoltsev, Y. Sharabi, M. Lyubarov, Y. Lumer, S. Tsesses, E. Lustig, I. Kaminer, and M. Segev, Light emission by free electrons in photonic time-crystals, Proc. Natl. Acad. Sci. U.S.A. **119**, e2119705119 (2022).
[45] Z. Gong *et al.*, Interfacial Cherenkov radiation from ultra-low-energy electrons, Proc. Natl. Acad. Sci. U.S.A. **120**, e2306601120 (2023).
[46] J. R. M. Saavedra, D. Castells-Graells, and F. J. Garcia de Abajo, Smith-Purcell radiation emission in aperiodic arrays, Phys. Rev. B **94**, 035418 (2016).
[47] R. Remez, N. Shapira, C. Roques-Carmes, R. Tirole, Y. Yang, Y. Lereah, M. Soljačić, I. Kaminer, and A. Arie, Spectral and spatial shaping of Smith-Purcell radiation, Phys. Rev. A **96**, 061801(R) (2017).
[48] I. Kaminer *et al.*, Spectrally and spatially resolved Smith-Purcell radiation in plasmonic crystals with short-range disorder, Phys. Rev. X **7**, 011003 (2017).
[49] J. D. Joannopoulos, S. G. Johnson, J. N. Winn, and R. D. Meade, *Photonic Crystals: Molding the Flow of Light* (Princeton University Press, Princeton, NJ, 2008).
[50] Z. V. Vardeny, A. Nahata, and A. Agrawal, Optics of photonic quasicrystals, Nat. Photonics **7**, 177 (2013).
[51] J. Veenstra, O. Gamayun, X. Guo, A. Sarvi, C. V. Meinersen, and C. Coulais, Non-reciprocal topological solitons in active metamaterials, Nature (London) **627**, 528 (2024).
[52] Y. Chen, R. Fleury, P. Seppecher, G. Hu, and M. Wegener, Nonlocal metamaterials and metasurfaces, Nat. Rev. Phys. **7**, 299 (2025).
[53] Z. Gong, R. Chen, Z. Wang, X. Xi, Y. Yang, B. Zhang, H. Chen, I. Kaminer, and X. Lin, Free-electron resonance transition radiation via Brewster randomness, Proc. Natl. Acad. Sci. U.S.A. **122**, e2413336122 (2025).
[54] P. W. Anderson, Absence of diffusion in certain random lattices, Phys. Rev. **109**, 1492 (1958).
[55] J. Billy, V. Josse, Z. Zuo, A. Bernard, B. Hambrecht, P. Lugan, D. Clément, L. Sanchez-Palencia, P. Bouyer, and A. Aspect, Direct observation of Anderson localization of matter waves in a controlled disorder, Nature (London) **453**, 891 (2008).
[56] A. Lagendijk, B. van Tiggelen, and D. S. Wiersma, Fifty years of Anderson localization, Phys. Today **62**, No. 8, 24 (2009).
[57] H. H. Sheinfux, Y. Lumer, G. Ankonina, A. Z. Genack, G. Bartal, and M. Segev, Observation of Anderson localization in disordered nanophotonic structures, Science **356**, 953 (2017).
[58] P. Wang, Y. Zheng, X. Chen, C. Huang, Y. V Kartashov, L. Torner, V. V Konotop, and F. Ye, Localization and delocalization of light in photonic moiré lattices, Nature (London) **577**, 42 (2020).
[59] A. Yamilov, S. E. Skipetrov, T. W. Hughes, M. Minkov, Z. Yu, and H. Cao, Anderson localization of electromagnetic waves in three dimensions, Nat. Phys. **19**, 1308 (2023).
[60] J. E. Sipe, P. Sheng, B. S. White, and M. H. Cohen, Brewster anomalies: A polarization-induced delocalization effect, Phys. Rev. Lett. **60**, 108 (1988).
[61] K. Y. Bliokh and V. D. Freilikher, Localization of transverse waves in randomly layered media at oblique incidence, Phys. Rev. B **70**, 245121 (2004).
[62] D. Zhang, W. Hu, Y. Zhang, Z. Li, B. Cheng, and G. Yang, Experimental verification of light localization for disordered multilayers in the visible-infrared spectrum, Phys. Rev. B **50**, 9810 (1994).
[63] X. Du, D. Zhang, X. Zhang, B. Feng, and D. Zhang, Localization and delocalization of light under oblique incidence, Phys. Rev. B **56**, 28 (1997).
[64] Y. Yamada, S. Takeuchi, S. Nitta, and S. Nonomura, Dependence of light propagation in random multilayers a-Si: H/a-Si_3N_{4+x}: H on incident angle, delocalization of p-polarized light and its explanation by extended Brewster angle: Experiments and simulation, J. Non. Cryst. Solids **198**, 796 (1996).
[65] A. A. Asatryan, L. C. Botten, M. A. Byrne, V. D. Freilikher, S. A. Gredeskul, I. V Shadrivov, R. C. McPhedran, and Y. S. Kivshar, Suppression of Anderson localization in disordered metamaterials, Phys. Rev. Lett. **99**, 193902 (2007).
[66] D. Mogilevtsev, F. A. Pinheiro, R. R. Dos Santos, S. B. Cavalcanti, and L. E. Oliveira, Suppression of Anderson localization of light and Brewster anomalies in disordered superlattices containing a dispersive metamaterial, Phys. Rev. B **82**, 081105 (2010).
[67] A. A. Fernández-Marín, J. A. Méndez-Bermúdez, J. Carbonell, F. Cervera, J. Sánchez-Dehesa, and V. A. Gopar, Beyond Anderson localization in 1D: Anomalous localization of microwaves in random waveguides, Phys. Rev. Lett. **113**, 233901 (2014).
[68] F. M. Izrailev and N. M. Makarov, Localization in correlated bilayer structures: From photonic crystals to metamaterials and semiconductor superlattices, Phys. Rev. Lett. **102**, 203901 (2009).
[69] A. G. Ardakani, Investigation of Brewster anomalies in one-dimensional disordered media having Lévy-type distribution, Eur. Phys. J. B **89**, 76 (2016).

[70] S. Kim and K. Kim, Disorder-enabled directional delocalization and wave steering in time-modulated dirac materials, Nanophotonics **15**, e70103 (2026).
[71] T. M. Jordan, J. C. Partridge, and N. W. Roberts, Nonpolarizing broadband multilayer reflectors in fish, Nat. Photonics **6**, 759 (2012).
[72] T. M. Jordan, J. C. Partridge, and N. W. Roberts, Suppression of Brewster delocalization anomalies in an alternating isotropic-birefringent random layered medium, Phys. Rev. B **88**, 041105(R) (2013).
[73] K. Y. Bliokh, Y. P. Bliokh, V. Freilikher, A. Z. Genack, B. Hu, and P. Sebbah, Localized modes in open one-dimensional dissipative random systems, Phys. Rev. Lett. **97**, 243904 (2006).
[74] K. Y. Bliokh, Y. P. Bliokh, V. Freilikher, S. Savel'ev, and F. Nori, Colloquium: Unusual resonators: Plasmonics, metamaterials, and random media, Rev. Mod. Phys. **80**, 1201 (2008).
[75] S. Rotter and S. Gigan, Light fields in complex media: Mesoscopic scattering meets wave control, Rev. Mod. Phys. **89**, 015005 (2017).
[76] K. Pichler, M. Kühmayer, J. Böhm, A. Brandstötter, P. Ambichl, U. Kuhl, and S. Rotter, Random anti-lasing through coherent perfect absorption in a disordered medium, Nature (London) **567**, 351 (2019).
[77] H. Cao, A. P. Mosk, and S. Rotter, Shaping the propagation of light in complex media, Nat. Phys. **18**, 994 (2022).
[78] M. V Rybin, D. S. Filonov, K. B. Samusev, P. A. Belov, Y. S. Kivshar, and M. F. Limonov, Phase diagram for the transition from photonic crystals to dielectric metamaterials, Nat. Commun. **6**, 10102 (2015).
[79] V. L. Ginzburg, *Transition Radiation and Transition Scattering* (A. Hilger, Bristol and New York, 1990).
[80] V. L. Ginzburg and I. M. Frank, Radiation of a uniformly moving electron due to its transition from one medium into another, J. Phys. (USSR) **9**, 353 (1945).
[81] J. Chen *et al.*, Low-velocity-favored transition radiation, Phys. Rev. Lett. **131**, 113002 (2023).
[82] R. Chen, J. Chen, Z. Gong, X. Zhang, X. Zhu, Y. Yang, I. Kaminer, H. Chen, B. Zhang, and X. Lin, Free-electron Brewster-transition radiation, Sci. Adv. **9**, eadh8098 (2023).
[83] K. Bliokh, Y. Bliokh, V. Freilikher, and F. Nori, Anderson localization of light in layered dielectric structures, in *Optical Properties of Photonic Structures: Interplay of Order and Disorder* (CRC Press, Boca Raton, 2012), pp. 57–86.
[84] P. Sheng and B. van Tiggelen, Introduction to wave scattering, in *Localization and Mesoscopic Phenomena* (Taylor & Francis, London, 2007).
[85] S. A. Gredeskul, Y. S. Kivshar, A. A. Asatryan, K. Y. Bliokh, Y. P. Bliokh, V. D. Freilikher, and I. V Shadrivov, Anderson localization in metamaterials and other complex media, Low Temp. Phys. **38**, 570 (2012).
[86] See Supplemental Material at http://link.aps.org/supplemental/10.1103/fkp4-9l19 for derivation of free-electron radiation from layered random nanostructures, localization length for layered random nanostructures, and more discussion on Brewster-anomaly-mediated free-electron radiation.
[87] S. Lowenthal and D. Joyeux, Speckle removal by a slowly moving diffuser associated with a motionless diffuser, J. Opt. Soc. Am. **61**, 847 (1971).
[88] X. Zhang, P. Chen, M. Li, Y. Shi, E. Hasman, B. Wang, and X. Chen, Brownian spin-locking effect, Nat. Mater. **25**, 207 (2026).
[89] F. Fan, S. Turkdogan, Z. Liu, D. Shelhammer, and C.-Z. Ning, A monolithic white laser, Nat. Nanotechnol. **10**, 796 (2015).
[90] S.-W. Chang, W.-C. Liao, Y.-M. Liao, H.-I. Lin, H.-Y. Lin, W.-J. Lin, S.-Y. Lin, P. Perumal, G. Haider, and C.-T. Tai, A white random laser, Sci. Rep. **8**, 2720 (2018).
[91] U. Keller, Recent developments in compact ultrafast lasers, Nature (London) **424**, 831 (2003).
[92] A. M. Weiner, *Ultrafast Optics* (John Wiley & Sons, New York, 2011).
[93] F. J. Rodríguez-Fortuño, G. Marino, P. Ginzburg, D. O'Connor, A. Martínez, G. A. Wurtz, and A. V Zayats, Near-field interference for the unidirectional excitation of electromagnetic guided modes, Science **340**, 328 (2013).
[94] X. Shi, X. Lin, I. Kaminer, F. Gao, Z. Yang, J. D. Joannopoulos, M. Soljačić, and B. Zhang, Superlight inverse Doppler effect, Nat. Phys. **14**, 1001 (2018).
[95] X. Chen, Y. Zhong, W. Ma, B. Zhang, H. Chen, T. Low, and X. Lin, Critical polarization suppression in the near-field interference of moving Huygens-like dipoles, Opt. Lett. **50**, 4562 (2025).
[96] V. L. Ginzburg, Some remarks on the radiation of charges and multipoles uniformly moving in a medium, Usp. Fiz. Nauk **172**, 341 (2002).
[97] Y. Shen, D. Ye, I. Celanovic, S. G. Johnson, J. D. Joannopoulos, and M. Soljačić, Optical broadband angular selectivity, Science **343**, 1499 (2014).

End Matter

To place our findings in the proper context, Fig. 4(a) captures the uniqueness of this Letter by mapping it onto a general phase diagram of reported interactions between free-electrons and random media. Three distinct regimes emerging in the phase diagram are illustrated by paradigmatic examples in Figs. 4(b)–4(j). The Brewster-anomaly delocalization for free-electron radiation uncovered in this Letter falls within the strong, unengineered-disorder regime [i.e., regime ① in Fig. 4(a)], which represents the general case of random media characterized by large disorder strength σ and arbitrary characteristic size d_0. In the equivalent dipolar-radiation picture, this regime is characterized by both random phases within a single realization and large phase variations under multiple realizations [Fig. 4(b)]. Remarkably, we show that in this regime free-electron radiation directionality remains robust against variations in both light frequency and particle velocity, manifesting as a persistent radiation peak at the Brewster

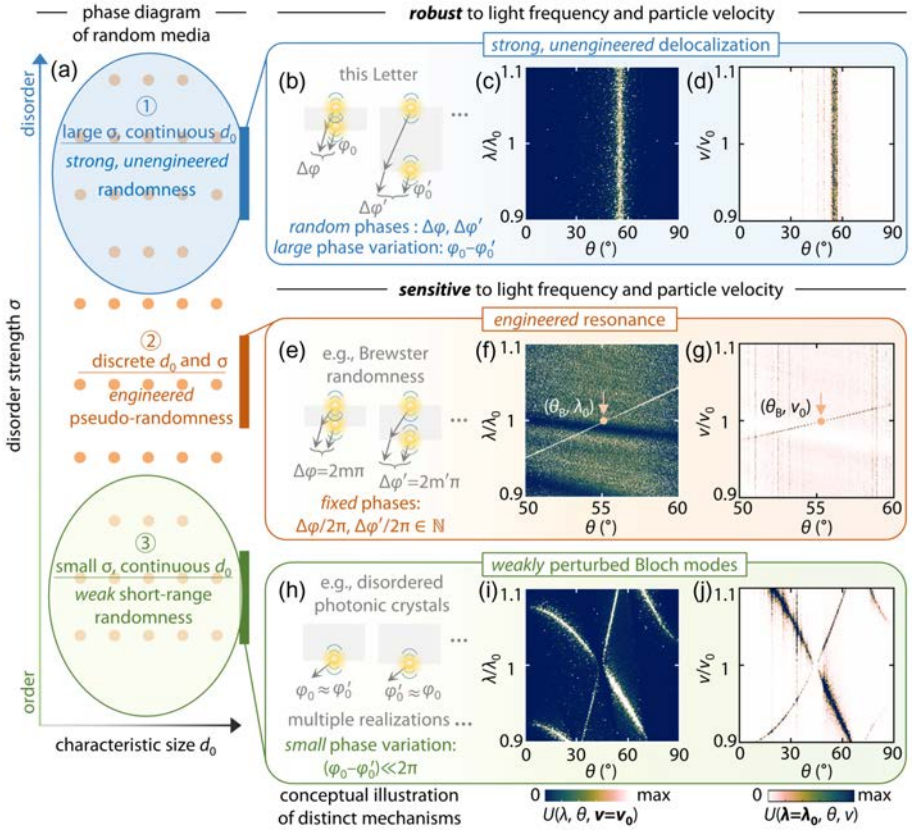


FIG. 4. Phase diagram of interactions between free-electrons and random media and their sensitivity to light frequency and particle velocity. (a) Phase diagram in the parameter space defined by characteristic size d_0 and disorder strength σ. (b)–(j) Underlying mechanisms and single-configuration angular spectral energy densities. By comparing two random configurations of a specific layer in (b), (e), and (h), distinct mechanisms are qualitatively distinguished by the phase differences between adjacent dipoles ($\Delta\varphi$ and $\Delta\varphi'$) within a single realization, and the variation in the initial dipole phases (φ_0 and φ_0') under multiple realizations. Intriguingly, only the strong, unengineered-disorder regime ① revealed in this Letter is robust to the variations in light frequency and particle velocity, shown by the vertical resonant lines in (c) and (d). The other conventional regimes include engineered-disorder regime ② in (f) and (g) and weak-disorder regime ③ in (i) and (j), where the free-electron radiations are distinguished by engineered resonances and weakly perturbed Bloch modes, respectively. For illustration, the Brewster-anomaly delocalization corresponds to strong, unengineered-disorder regime in (b)–(d), where $N = 50\,000$. The so-called Brewster randomness [53] corresponds to engineered-disorder regime in (e)–(g), where $N = 5000$ and each layer thickness is a random odd multiple (e.g., discretely and uniformly distributed among $1, 3, 5, \ldots, 19$) of a basic value. Disordered photonic crystals [45] correspond to weak-disorder regime in (h)–(j), where $N = 50\,000$ and each layer thickness follows a continuous uniform distribution over $[0.98\lambda_0, 1.02\lambda_0]$. All other structural setups in (b)–(j) are the same as those in Fig. 2.

angle [Figs. 4(c) and 4(d)]. This robustness is rooted in the fact that Brewster-anomaly delocalization for free-electron radiation does not rely on structural resonance. Meanwhile, the value of the Brewster angle is independent of particle velocity and can remain consistent over a broad spectrum for nondispersive constituent dielectrics, which are abundant in nature [97].

The robustness also distinguishes our findings from previously reported forms of free-electron radiation that are invariant to structural randomness. In the engineered-disorder regime [i.e., regime ② in Fig. 4(a)], the structural variation is pseudorandom. Specifically, the fundamental distinction between the strong, unengineered-disorder regime and engineered-disorder regime lies not in the disorder strength, but in whether the underlying randomness is discrete or continuous. For example, in the case of the so-called Brewster randomness [53] shown by a set of discrete points spanning the full range from weak to strong disorder in Fig. 4(a), only a discrete set of layer thicknesses—integer multiples of a specific value—is permitted, which locks the phase coherence [Fig. 4(e)]. Since this fixed phase coherence is easily disrupted by the variations in light frequency and particle velocity, the resulting free-electron radiation based on engineered resonances is highly sensitive [Figs. 4(f) and 4(g)]. Finally, a more conventional weak-disorder regime [i.e., regime ③ in Fig. 4(a)] exists in weakly perturbed periodic systems, such as metamaterials or photonic crystals with short-range randomness introduced by fabrication

imperfections. In such systems, the phase variation is so small [Fig. 4(h)] that free-electron radiation is still governed by the Bloch-mode dispersion and thus remains sensitive to the light frequency and electron velocity [Figs. 4(i) and 4(j)]. From an alternative perspective, the contrast between free-electron radiation in the weak-disorder regime and the strong, unengineered-disorder regime suggests a disorder-immune pathway via the Brewster effect to overcome the inherent chromaticity (i.e., frequency dependence) of light emission from photonic crystals.